Effect of modified graphene oxide on Cu and phosphorus in eutrophic river sediments

Zhipeng Lin, Lei Song, Baohong Han, Hao Li and Qian Wang

ABSTRACT

Ulansuhai nur is located in the cold and dry area of China, and the management of heavy metals in the sediments is related to water safety in the lower places of the Yellow River. Graphene oxide (GO) is modified to obtain magnetic graphene oxide (G-F) and chitosan grafted graphene oxide (G-N-C) materials, which are used to immobilize Cu in the sediments. The modified materials are characterized by scanning electron microscopy (SEM), Fourier transform infrared spectroscopy (FTIR), and X-ray diffractometer (XRD). G-F respectively reduces the concentration of Cu in the overlying and interstitial water by 61.5–66.3% and 22.4–47.1%, which is more effective than GO and G-N-C. Experiments are designed to determine the effect of phosphates concentration on immobilizing Cu in the sediments by modified materials. The results show that a low concentration of phosphates solution is beneficial to the immobilization of Cu in the sediments, and the capability of G-F to immobilize Cu is higher than that of GO and G-N-C. G-F presents a lower increase in organic phosphorus in the sediments than GO and G-N-C. In summary, the modified materials can immobilize Cu in the sediments, potentially reduce the water body eutrophication, and improve the lake ecological environment.

Key words | concentration of phosphates, immobilization, modified graphene oxide, sediments

Zhipeng Lin
Lei Song (corresponding author)
Qian Wang
Department of Municipal Engineering, School of Civil Engineering,
Inner Mongolia University of Technology,
Hohhot, Inner Mongolia, 015400,
China
E-mail: *songlei2013@imut.edu.cn*

Baohong Han
Department of Municipal and Environmental Engineering, School of the Civil Engineering,
Beijing Jiaotong University,
Beijing, 10000,
China

Hao Li
China Mobile Group Shandong Co., Ltd, Jinan,
Shandong, 250000,
China

HIGHLIGHTS

- Graphene oxide (GO) is modified through different modification methods.
- Magnetic graphene oxide (G-F) immobilizes Cu with high efficiency.
- Modified materials reduce the concentration of Cu in the overlying and interstitial water.
- Low-concentration phosphates helps the modified materials immobilize Cu.
- G-F plays a positive role in the treatment of water eutrophication.

doi: 10.2166/wst.2020.390

GRAPHICAL ABSTRACT

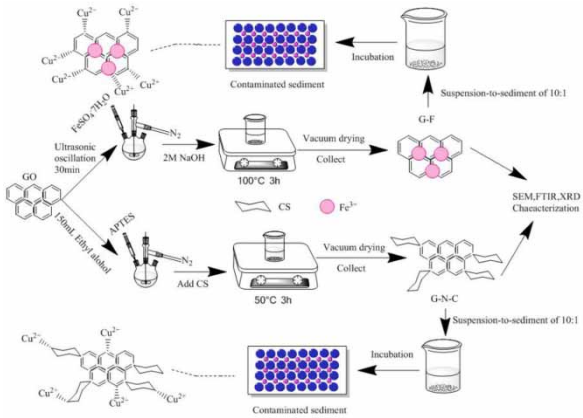

INTRODUCTION

With the acceleration of industrialization, a large number of heavy metals are discharged into lakes through atmospheric deposition, surface runoff, and waste water, and most heavy metals enter the sediments. If the water environment changes, heavy metals in the sediments would be released again, which would be a serious threat to the ecological environment (Yan *et al.* 2016). According to another survey, the sediments of lakes and rivers in China have been seriously polluted by heavy metals (Jiang *et al.* 2018). Therefore, it is an urgent problem to find stable and efficient adsorbents to immobilize heavy metals in the sediments.

In recent years, graphene oxide (GO) has exhibited good water dispersibility and biocompatibility due to its effective oxygen-containing functional groups, such as hydroxyl, carboxyl and epoxy groups on the surface. These properties could be effectively used for the adsorption of heavy metal ions and dyes (Ahmad *et al.* 2019). However, the small particle size and easy aggregation features of GO caused an unsatisfactory immobilizing effect (Ramesha *et al.* 2011). Therefore, researchers prefer to immobilize heavy metals by modifying GO. At present, the modification processes can be divided into four methods, which are physical, chemical, magnetic modification and impregnation (Zhao *et al.* 2019). Among them, chemical modification and magnetic coating are the most widely used methods. Magnetic coating could enhance the specific surface area of GO, and increase the efficiency of modified materials to immobilize heavy metals (Shraban *et al.* 2020). The composite of Fe_3O_4 and graphene oxide shows excellent adsorption capacity for Pb (Hu *et al.* 2017). GO with Fe_3O_4 loaded on the surface can improve the electron transfer between metal oxides and organic materials, and adsorb heavy metals more efficiently than GO (El-Shafai *et al.* 2020). Chemical modification can positively change the number and type of functional groups on the surface of GO. Amine functionalization introduces ammonia ions into GO surface, which can enhance GO's electronegativity and allow it to adsorb heavy metal ions more efficiently (Wang *et al.* 2018). In addition, chitosan-modified GO has higher adsorption capability for heavy metals, a wider pH range, and stronger adaptability to the environment than GO (Cao *et al.* 2019). From this point of view, both magnetic and chemical modification can improve the efficiency of GO to immobilize heavy metals. Researchers have paid more attention to the treatment of heavy metals and organic pollutants in water (Liu *et al.* 2019b). However, due to the lack of research on the stable solidification of heavy metals in the sediments, researchers have been insufficiently aware of the effects of modified materials on immobilizing heavy metals in the sediments.

Generally, released excessive phosphorus into water body would cause eutrophication and reduce the concentration of dissolved oxygen (DO) in water (Jin *et al.* 2019). As a typical grassland lake in the cold and arid regions, Ulansuhai nur has arid regional climatic conditions, where rainwater dilution and the purification capability of the environment cannot offset the damage of external pollutants to the ecosystem. Heavy metals contamination and

eutrophication in the sediments have increased in Ulansuhai nur year by year. Nitrogen and phosphorus in overlying water affect the immobility of heavy metals in the sediments to some extent (Rinklebe *et al.* 2016b). Phosphates can immobilize heavy metals in the sediments. However, the effect of immobilization depends on the available phosphorus content in the soil or sediments, as soluble phosphorus performed considerably better than insoluble phosphorus in the process of restoration (Su *et al.* 2015). Nutrients (such as N, P, and S) changed the distribution of microbial communities in the sediments of the Bohai Sea in China, which in turn adversely influenced the immobility of heavy metals in the sediments (Lu *et al.* 2019). A study has also shown that heavy metals (such as As, Ba, Cd, Cu, Pb, and Sr) in the sediments may be released under aerobic conditions (Rinklebe *et al.* 2016b), which is inconsistent with previous research. When the pH and oxidation–reduction potential (ORP) change in the sediments, heavy metals may reenter the overlying water and cause secondary pollution (Rinklebe *et al.* 2016a). Therefore, it is of great significance to study the influence of modified materials on the immobilization of heavy metals by simulating the changes of water environment.

In this paper, by changing the type and number of oxygen-containing functional groups on the surface of GO and optimizing its specific surface area, two modified materials were prepared to immobilize Cu in the Ulansuhai nur sediments and reduce the ecological risk of Cu. In the present study, we compared the effect of G-F with that of G-N-C on immobilizing Cu in the sediments; we designed the experiments based on the actual situation of severe eutrophication in Ulansuhai nur in recent years, studied the immobilization effect of the modified materials on copper under different environmental conditions, and initially analyzed the immobilization mechanism. This study may help to understand the influence of water environment changes on heavy metals immobilization in the sediments.

MATERIALS AND METHODS

Preparation and characterization of GO loaded with Fe_3O_4 (G-F)and GO grafted with chitosan (G-N-C)

Preparation of G-F

GO (0.05 g) was added to 50 mL of deionized water and sonicated for 30 min to form a GO suspension. Subsequently, 0.5 g of $FeSO_47H_2O$ was accurately weighed and added into 2.5 mL of deionized water. 2 mol L^{-1} NaOH was prepared, and added into the $FeSO_4$ solution. The mixed solution was then added into the GO suspension and ultrasonically shaken for 30 min to allow the reaction to proceed fully. The obtained mixture was heated to reflux at reflux temperature for 3 h, then filtered by a quantitative filter paper. The filtered matter was dispersed in an acetone solution, and finally dried at 180 °C overnight.

Preparation of aminated G-N-C

GO (0.3 g) was dispersed in 150 mL of ethanol and sonicated for 30 min at room temperature. Subsequently, 2.3 mL of 3-aminopropyl triethoxysilane (APTES) was added drop-wise into the GO suspension in N_2 atmosphere. Then the mixture was stirred and maintained at reflux temperature for 24 h. The filtered materials were washed five times with ethanol, and finally dried to obtain aminated graphene oxide (G-N).

0.5 g chitosan (CS) was dissolved in 10 mL 1% (v/v) acetic acid solution, and 1 g G-N was slowly added into the CS solution. The mixture was magnetically stirred for 10 min, then slowly heated to 50 °C, and stirred for 3 h. The final mixture was washed several times with acetone and filtered by a quantitative filter paper; the filtered materials were dried *in vacuo* to obtain G-N-C.

Characterization of GO, G-F, and G-N-C

Scanning electron microscopy (SEM) images of GO, G-F and G-N-C were obtained using field emission environment SEM (FEI QUANTA 650 FEG). Fourier transform infrared spectroscopy (FTIR) (Thermo Nicolet-870 spectrophotometer) was used to record the FTIR spectra of GO, G-F and G-N-C, which ranged from 400 cm^{-1} to 4,000 cm^{-1}. X-ray diffraction (XRD) patterns were retrieved using an X-ray diffractometer (RigakuD/max-2550 VK/PC diffractometer equipped with Cu Ka radiation at 40 kV and 40 mA) to verify the crystal structures of GO, G-F and G-N-C.

Experimental design

Sediments treatment with GO, G-F and G-N-C

In this experiment, sediment sampling points and determination of the total amount of Cu were placed in an externally specified index (ESI). Cu was repaired by GO, G-F and G-N-C *in situ*. A total of 16 G-point sediment samples (10.000 ± 0.005 g) were accurately weighed. Four experimental design groups and a control group (10 g air-

dried precipitate only) were investigated. The test groups included GO group [10 g air-dried precipitate, 5, 10, and 15% (w/w) GO], G-F group [10 g air-dried precipitate, 5, 10 and 15% (w/w) G-F], and G-N-C group [10 g air-dried precipitate, 5, 10 and 15% (w/w) G-N-C]. Each sample was placed in a 150 mL vial with 100 mL of deionized water. Three replicates were carried out for each experimental group. The samples were then incubated at room temperature for 35 days. The BCR extraction was done at the 1st, 3rd, 7th, 15th, 25th and 35th day. The concentrations of Cu in the overlying and interstitial water were measured at the 35th day.

Effects of different concentrations of phosphorus in the overlying water on Cu immobilization by GO, G-F and G-N-C

A total of 16 G-point precipitation samples (10.000 ± 0.005 g) were accurately weighed and placed in a 250 mL beaker, respectively. Subsequently, they were divided into four groups: one 200 mL deionized water group, and three sodium phosphate solution (0.025, 0.5 and 1 mgL^{-1}) groups. The deionized water group was taken as a control group. An amount of 15% (w/w) of GO, G-F and G-N-C were respectively added into the other three groups. Then, the samples were kept in a hermetic space for 35 days. The experimental designs were repeated three times. Concentration of phosphorus, available phosphorus, pH, ORP and DO values in the overlying water were measured at the 1st, 3rd, 7th, 15th, 25th and 35th day. Finally, the BCR extraction was performed.

RESULTS AND DISCUSSION

Characterization of GO, G-F and G-N-C

Figure 1(a) presents the typical wrinkled layered structure of GO. Figure 1(b) shows that Fe_3O_4 loaded on GO surface significantly increased the specific surface area of GO, which improved the adsorption sites for Cu. Figure 1(c) displays the grooves on the surface of G-N-C based on the different stiffnesses between chitosan and GO. Comparing with GO (in Figure 1(a)), the mass density of G-N-C (in Figure 1(c)) significantly increased, which indicated that GO and CS were coupled.

GO, CS, G-N, G-N-C and G-F composites were described by FTIR analysis. As shown in Figure 2(b), the –OH, C = O, $–NH_2$ and C–OH vibrations respectively occurred at 3,390, 1,720, 1,620 and 1,050 cm^{-1} in GO spectrum (Yadav *et al.* 2014). In Figure 2(a), –OH at 3,390 cm^{-1} moved to a high frequency, which indicated an enhancement of the hydrogen bonding between Fe_3O_4 and GO. $–CH_2$ vibration occurred at 2,880 cm^{-1}. The tensile vibrations of C–C, C–O and C = C were evident at 1,000–1,500 cm^{-1} (Yan *et al.* 2016), and the C = O bond at 1,720 cm^{-1} moved to 1,600 cm^{-1}, forming $–COO^-$ (Song *et al.* 2017). G-F vibration at 604 cm^{-1} was attributed to the Fe–O group (Yan *et al.* 2016), which demonstrated that

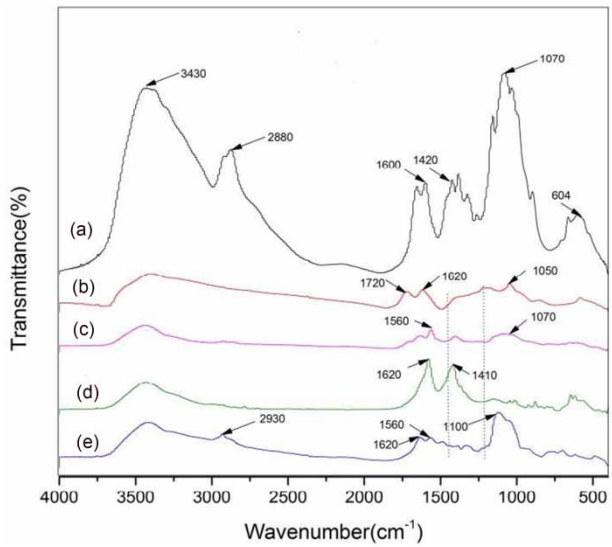

Figure 2 | (a) FTIR spectra of G-F, (b) GO, (c) G-N, (d) CS, (e) G-N-C.

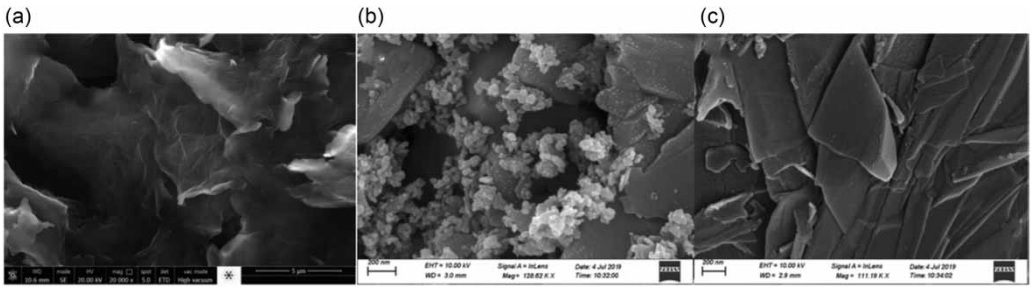

Figure 1 | SEM image of (a) GO, (b) G-F SEM image, (c) G-N-C SEM image.

Fe_3O_4 was loaded on the GO surface. In Figure 2(c), the C = O peak at 1,720 cm^{-1} disappeared, and the $-NH_2$ at 1,620 cm^{-1} moved to 1,560 cm^{-1}. At the same time, the peak of C–OH at 1,070 cm^{-1} further widened (Sun *et al.* 2019). As shown in Figure 2(d), –OH vibration at 3,420 cm^{-1}, $-NH_2$ peak at 1,620 cm^{-1}, and C–O vibration at 1,410 cm^{-1} were evident in the FTIR spectrum of CS. As shown in Figure 2(e), the broad peak at 3,430 cm^{-1} was ascribed to the presence of –OH and $-NH_2$. The characteristic peak of –CH bond appeared at 2,930 cm^{-1}, while the C–OH bond was evident at 1,100 cm^{-1}. The change at 1,470–1,270 cm^{-1} described the stretching of the C–N bond and the bending of the NH_2 and $-NH^-$ groups (Zhuang *et al.* 2009). Hence, the new material G-N-C was successfully made.

Structural analyses of GO, CS powder, G-F and G-N-C composites were conducted via XRD ($2\theta = 10°–90°$). As shown in Figure 3(a), 26.42° was the characteristic diffraction peak of GO, which corresponded to the 002 plane and exhibited narrow and strong features. For G-F composites in Figure 3(c), new diffraction crystalline peaks appeared at $2\theta = 18.31°$, 30.121°, 35.479°, 53.495°, 57.026° and 62.622° respectively, corresponding to 111, 220, 311, 422, 511 and 440 (Zhang *et al.* 2019b). These results indicated that Fe_3O_4 had been successfully loaded on the GO surface. In Figure 3(b), the characteristic peak of CS appeared at $2\theta = 25.726°$ due to its amorphous structure (Samuel *et al.* 2019). As shown in Figure 3(d), the characteristic peaks of CS and GO respectively occurred at $2\theta = 25.726°$ and $2\theta = 26.42°$. Therefore, certain GO and CS with amorphous structures were presented. Moreover, physical graft exchange between CS and GO might occur (Song *et al.* 2017).

Sequential extraction of Cu

The total amount of Cu in the sediments was 55.6 mg kg^{-1}. Heavy metals in the sediments could be divided into four different forms (acid soluble form, reducible form, oxidizable form, residual form), and the aforementioned four forms of heavy metals were interconvertible in the sediments. Figure 4 shows the composition changes of Cu in the sediments of GO, G-F and G-N-C. GO, G-F and G-N-C had different mass fractions.

Figure 4(a) clearly shows that the migration and conversion capacity of Cu significantly decreased when stable materials were added at the 35th day. Comparing with the result in the blank test (without GO, G-F and G-N-C), the

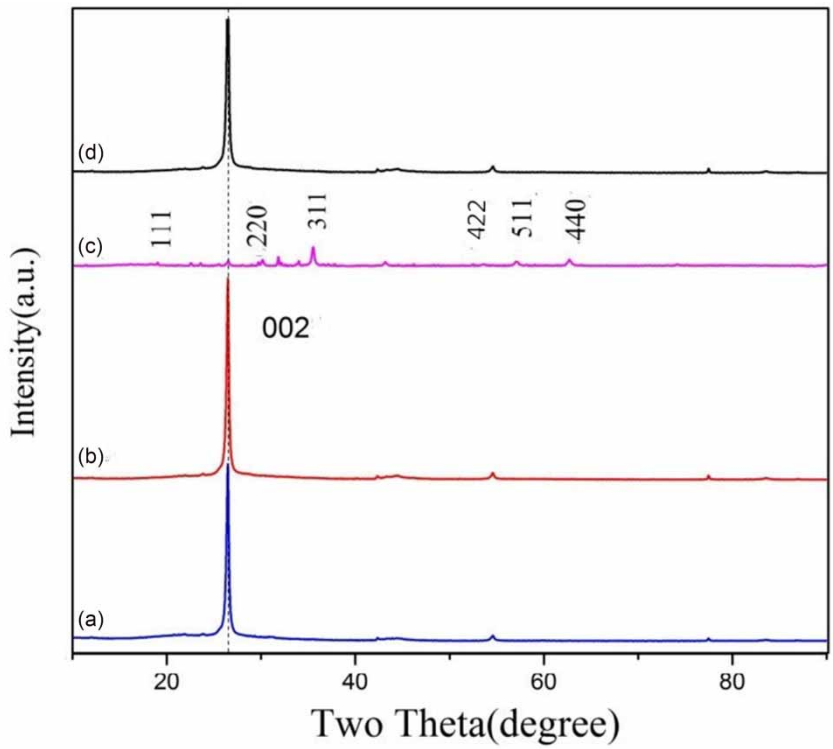

Figure 3 | XRD map of (a) GO, (b) CS, (c) G-F, (d) G-N-C.

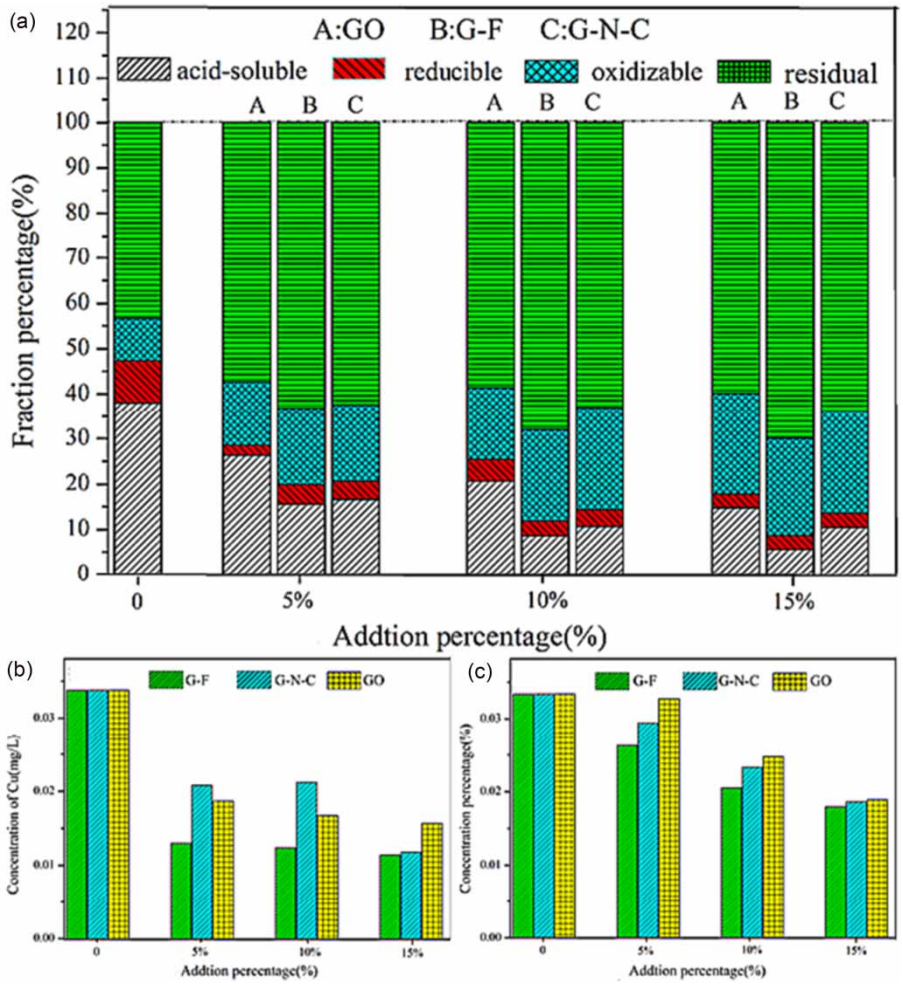

Figure 4 | (a) Effect of different GO, G-F, G-N-C dosages (5, 10, 15 wt%) on the morphological content of Cu in sediments with aging time, (b) surface water and (c) concentration of heavy metal Cu in interstitial water under. different GO, G-F, G-N-C dosages (5, 10, 15 wt%).

acid extractable state respectively decreased by 7.76%, 13.36% and 19.28% after adding 5, 10 and 15% of GO. With an increased amount of GO, the residual state also slightly changed. Besides, comparing with the result in the control group, when 5, 10 and 15% of G-F were respectively added, the acid extractable state respectively decreased by 22.42, 29.35 and 32.36%, while the residual state respectively increased by 19.77, 26.38 and 26.49%. In addition, after adding 5, 10 and 15% of G-N-C, the acid extractable state respectively decreased by 21.42, 27.37 and 27.5%, while the residual state respectively increased by 19.02, 19.63 and 19.99%. The experimental results clearly showed that the acid extractable portion of Cu exhibited different reduced levels when the mass fractions of the three stable materials (i.e. GO, G-F and G-N-C) increased. Moreover, the residual state increased with an increase in mass fraction of the dosing stabilizer. The above mentioned three stable materials had the best ability for immobilizing Cu at 15% quality score.

Figure 4(a) exhibits that the order, in ability, for immobilizing Cu was G-F > G-N-C > GO when the added amounts of GO, G-F and G-N-C were approximately 15 wt%. The FTIR spectrum shows a large number of carboxyl and hydroxyl groups in G-F. The SEM indicates that Fe_3O_4 was embedded on the GO surface, which increased the specific surface area of GO and provided abundant adsorption sites for immobilizing Cu. Both FTIR and SEM demonstrate that CS-grafted GO increased the type of high-quality functional groups on the GO surface, while it did not expand the specific surface area of the GO. Therefore, the efficiency of G-F for immobilizing Cu was excellent due to an increase in specific surface area of G-F.

Moreover, the oxygen-containing functional groups present on the surface of G-F accelerate the ion exchange between Cu and stable materials. Hence, the bioavailability of Cu was reduced and the Cu was immobilized in the deposit.

The concentration of Cu in overlying and interstitial water

Figure 4(b) and 4(c) illustrate the concentration of Cu in overlying and interstitial water. In the control group (without GO, G-F and G-N-C), the concentration of Cu in overlying and interstitial water were respectively 0.033 mg L^{-1} and 0.034 mg L^{-1}. The concentration of Cu in the overlying and interstitial water significantly decreased with an increase in the mass fractions of GO, G-F and G-N-C. When the stable materials with mass fractions of 5, 10 and 15% were added, the Cu content in overlying and interstitial water may be arranged in descending order as time increases: G-F> G-N-C> GO. Comparing with the result in the control group (without GO, G-F and G-N-C), the concentration of Cu in overlying and interstitial water respectively reduced by 44.6–53.5% and 3–42.7%. In the G-N-C experimental group, the concentration of Cu in overlying and interstitial water respectively reduced by 38.5–65% and 14.4–45.4%. In the G-F experimental group, the concentration of Cu in overlying and interstitial water respectively decreased by 61.5–66.3% and 22.4–47.1%. The exchange in soluble contaminants between the sediments and overlying water could be achieved through the interstitial water, and biological toxicity was closely related to the interstitial water. G-F excelled in reducing the concentration of Cu in overlying and interstitial water. Comparing with GO and G-N-C, G-F was more effective in reducing the risk of Cu being released back into the overlying water.

Distribution of metal forms in the sediment samples under the change of the concentration of phosphorus in overlying water

Previous studies indicated that phosphate compounds could effectively immobilize heavy metals such as Pb, Cd, Cu and Zn. However, phosphates in overlying water changed the DO of water, and the Ph and ORP of the sediments, which directly increased the ecological risk of heavy metals (Banks *et al.* 2012). In this study, three stable materials (GO, G-F and G-N-C) were added to investigate their effect on immobilizing Cu under different concentrations of phosphorus-containing overlying water.

The results in the control group in Figure 5 show that the stability of Cu continuously decreases as the concentration of phosphates in the overlying water increases (0.25, 0.5, and 1 mg L^{-1}). In the experimental group, when deionized water was added for aging for 35 days, the phosphate concentration in the overlying water was lower than the limit. The residual state of the GO group increased by 6.77%, while the acid extractable state decreased by 12.28%. The residual state of the G-F group increased by 10.36%, and the acid extractable state decreased by 13.37%. The residual state of the G-N-C group increased by 7.12%, while the acid extractable state decreased by 12.77%. When the concentration of phosphates in the overlying water was 0.25 mg L^{-1}, the residual state in the GO group increased by 8.68%, while the acid extractable state decreased by 16.56%. The residual state in the G-F group increased by 16.76%, while the acid extractable state decreased by 20%. The residual state in the G-N-C group increased by 15.89%, while the acid extractable state decreased by 18.89%. When the concentration of phosphates in the overlying water was 0.5 mg L^{-1}, and the aging time was 35 days, the residual state of the GO group increased by 10.25%, while the acid extractable state decreased by 12.3%. The residual state of the G-F group increased by 13.76%, while the acid extractable state decreased by 13.02%. The residual state in the G-N-C group increased by 12.5%, while the acid extractable state decreased by 12.89%. When the concentration of phosphates in the overlying water was 1 mg L^{-1}, and the aging time was 35 days, the residual state of the GO group increased by 12.5%, while the acid extractable state decreased by 12.3%. The residual state of the G-F group increased by 15.78%, while the acid extractable state decreased by 15%. In the G-N-C group, the residual state increased by 15.01%, while the acid extractable state decreased by 13.89%. Hence, prolonging the aging time led to a high concentration of phosphates in the overlying water and high bioavailability of Cu. The researchers also found a similar pattern in a previous study, and concentration of phosphates was closely related to the mobility of heavy metals (Liu *et al.* 2019a). After adding identical amount of GO, G-F and G-N-C, with an increase in the concentration of phosphates in the overlying water, the efficiencies for immobilizing Cu by the three materials increased at the 35th day. Moreover, the efficiency for immobilizing Cu by G-F was higher than those of GO and G-N-C.

Perhaps the Cu in the overlying water may form soluble heavy metal phosphates. Figure 6 shows that the total

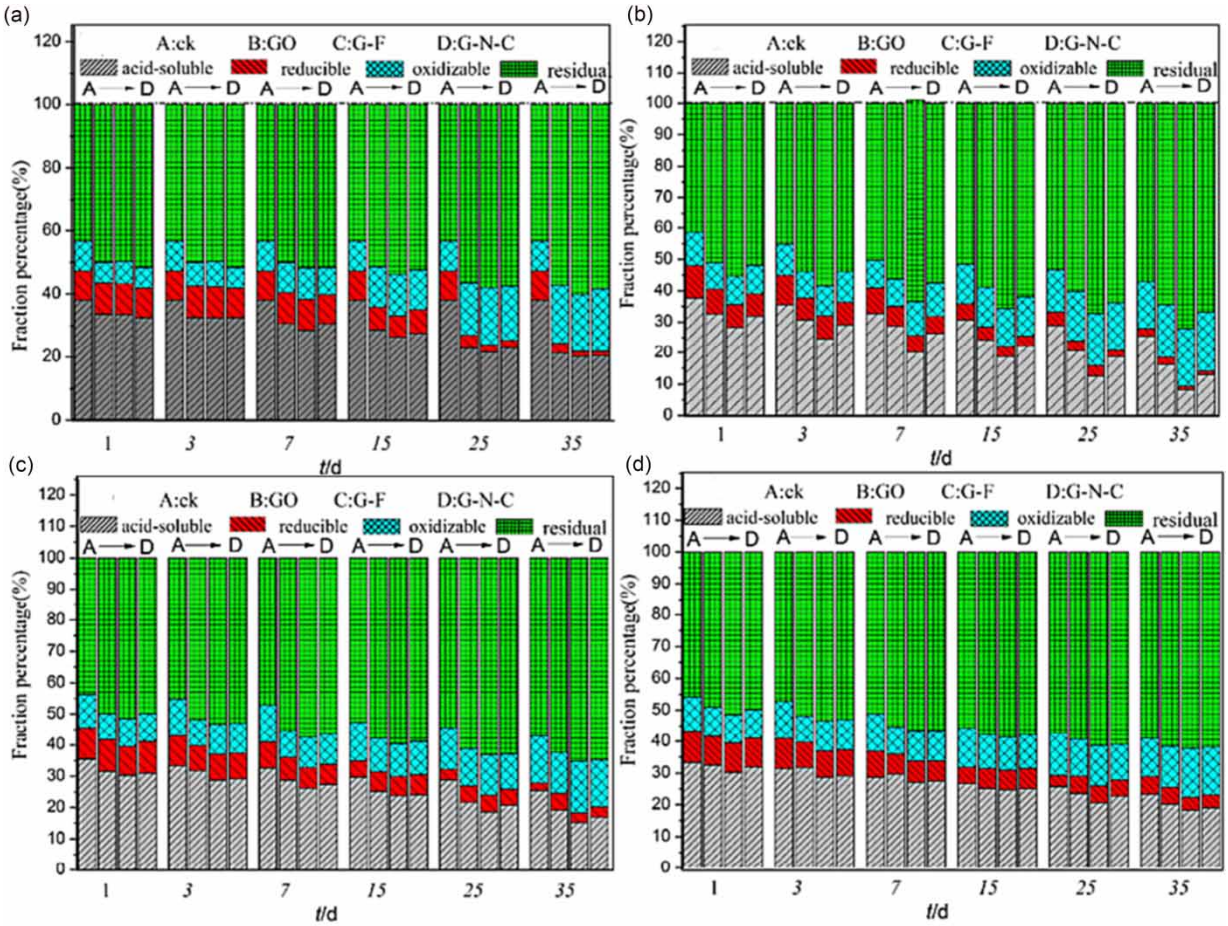

Figure 5 | Addition of GO, G-F, and G-N-C to (a) deionized water (0 mg L^{-1}) and different concentrations of phosphate solution [(b) 0.25, (c) 0.5, (d) 1 mg L^{-1}] affects the distribution of Cu and changes with the aging time.

phosphorus (TP) in the overlying water gradually decreased in the control group, whereas the available phosphorus in the sediments gradually increased. The above-mentioned trend was also evident in the three experimental groups, which may be explained by the preceding discussion. The phosphates in the overlying water were held by the deposit, forming a metal phosphate with Cu, the metal phosphate precipitating in the sediments. Comparing with the results in control groups, the content of available phosphorus in the sediments increased by 94–124 mg kg^{-1} after adding GO, and the content of available phosphorus in the sediments increased by 63–115 mg kg^{-1} after adding G-F. Moreover, after adding G-N-C, the content of available phosphorus in the sediments increased by 106–126 mg kg^{-1}. Comparing with G-N-C and GO groups, the increase in amount of available phosphorus in the sediments after the addition of G-F was small. Because of the large amount of iron present in the G-F, the iron might precipitate with phosphates, which reduced the available phosphorus content (Gil-Diaz *et al.* 2016). Thus, a large amount of phosphates was adsorbed in the G-F. The reaction between iron oxide and the phosphate anion could be expressed by Equation (1).

$$FeOOH + HPO_4^{2-} \rightarrow FeOHPO_4^{-} + OH^{-} \quad (1)$$

Anion-induced adsorption and changing the negative charge of the adsorbent surface were the main mechanisms for immobilizing cations (such as Pb, Cu, Cd, Cr, etc) (Sanderson *et al.* 2016). Studies had shown that the presence of PO_4^{2-} strengthened the adsorption of Pb on metal oxides, which might be related to co-adsorption. There were two reasons for co-adsorption, the first being related to the formation of surface ternary complexes, and the other being electrostatic attraction between positively charged Pb^{2+} and negatively charged PO_4^{2-}. (Zhao *et al.* 2016). As shown

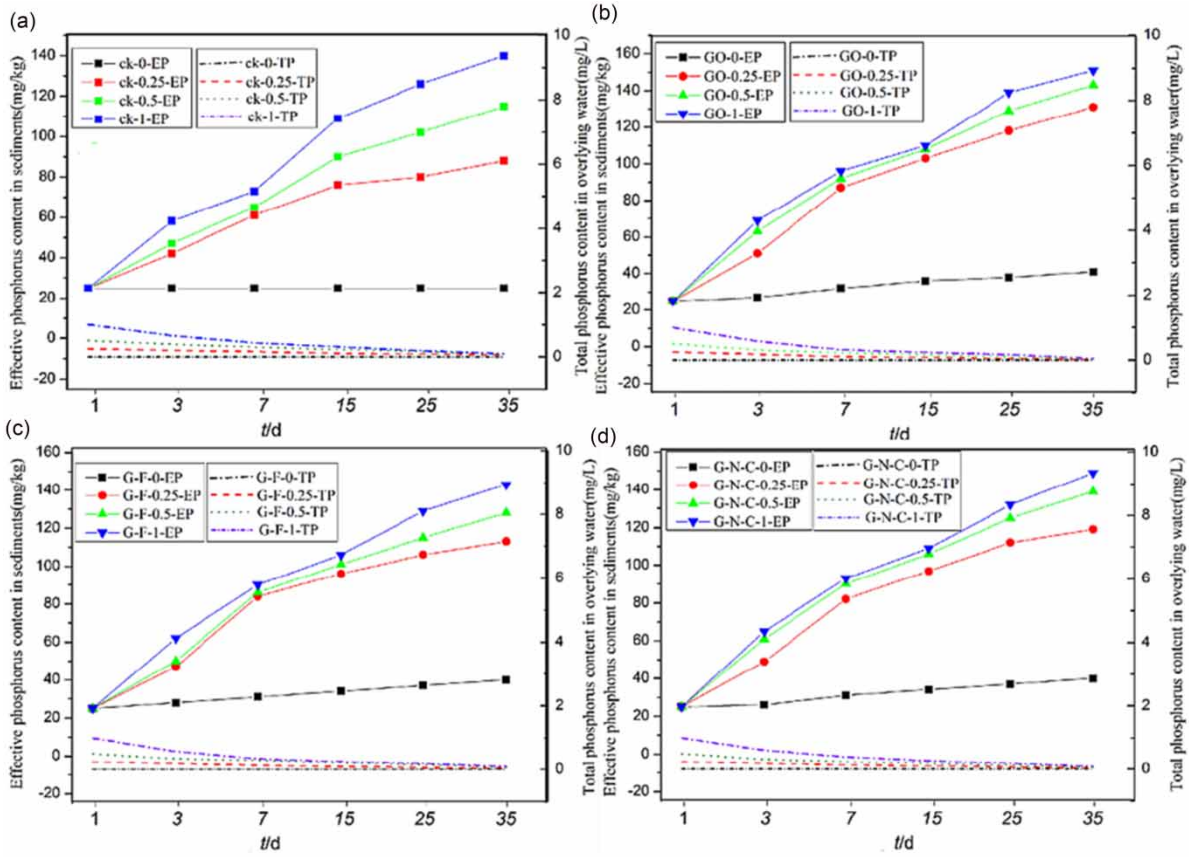

Figure 6 | Addition of different adsorbents (G-O, G-F, and G-N-C), changes in available phosphorus and TP in deionized water (0 mg L^{-1}) and different concentrations of phosphate solution [0.25, 0.5, and 1 mg L^{-1}; (a) ck, (b) GO, (c) G-F, (d) G-N-C].

in Figures 5 and 6, the increase in available phosphorus after adding GO and G-N-C was more notable than that under G-F; however, the effect for immobilizing Cu by GO or G-N-C was worse than that by G-F. Maybe the competitive adsorption for Cu between phosphates and stabilizer in the overlying water occurred after adding GO and G-N-C. Cu and phosphates formed unstable metal phosphates, which weakened the immobilization effect for Cu. When iron oxide was used to remove Pb and PO_4^{2-} in water at the same time, iron oxide would first form complexes with Pb, and then these complexes would act as adsorption materials to further adsorb PO_4^{2-} in water (Shi *et al.* 2020). Similar to Pb, phosphates had a good adsorption capacity for Cu (Zeng *et al.* 2017). Phosphate could form phosphate complexes with Cu, these complexes were insoluble in water, but soluble in ammonia, dilute acid and ammonium salt solution. In recent years, due to the inflow of external pollutants, the pH value of Ulansuhai nur had significantly changed, which would increase the possibility of copper phosphates in the sediments being re-released in the overlying water, causing harm to the ecological environment. After adding the stable materials, Cu could complex with the iron oxide on the surface of the G-F, thereby forming a more efficient adsorption material to adsorb PO_4^{2-}. G-F shows good performance in the aspect of immobilizing Cu and adsorbing phosphates.

The experiment also measured the DO concentration of the overlying water, and the pH and ORP values of the sediments. At the same concentration of phosphates in the overlying water after 35 days of aging, Figure 7(b) shows that the pH value of the experimental group increased compared with the control group. In the experimental group, as the concentration of phosphates in the overlying water increased, the pH value in the original sediments was lower than that in the sediments after adding deionized water. At a concentration of phosphates in the overlying water of 0.25 mg L^{-1}, after adding GO, G-F and G-N-C stabilizers, comparing with the deionized water group, the

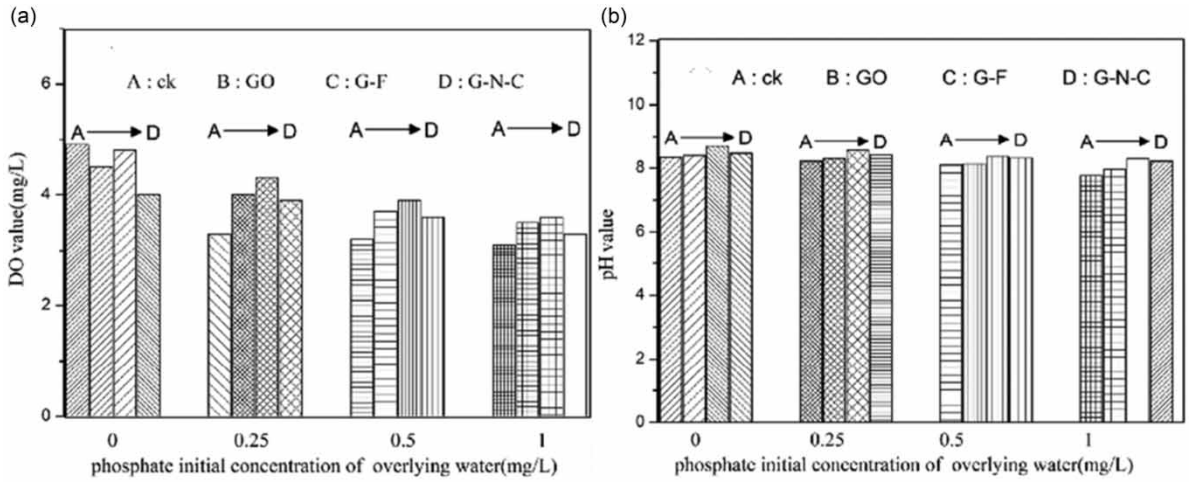

Figure 7 | Addition of GO, G-F, and G-N-C to deionized water (0 mg L^{-1}) and different concentrations of phosphate (0.25, 0.5, and 1 mg L^{-1}) affect the change of DO, pH in sediments [(a) DO, (b) pH].

decreased level in pH of the sediments was smallest when G-F was added. The sediments' ORP value in Figure S2 shows an opposite trend. This may be because the phosphates were unstable in the aqueous solution. In addition, under the weak alkaline conditions, HPO_4^{2-} would be hydrolyzed and release H^+, which lowered the pH of the sediments. Increasing concentration of phosphates in the overlying water will cause a decrease in the pH value of the sediments. Generally, increasing pH value is beneficial for the adsorption and co-precipitation of Cu and metallic iron ore. In addition, G-F will reduce the possibility of HPO_4^{2-} forming unstable metal phosphates with Cu. Therefore, the effect of G-F on immobilizing Cu was better than that of GO and G-N-C.

The DO concentration in the overlying water confirmed the superior immobilizing capability of G-F for Cu. When the concentration of phosphates in the overlying water was identical after 35 days, Figure 7(a) shows that the dissolved oxygen gradually increased compared with the control group. In the low oxygen state, phosphates were commonly adhered to the surface of the deposit (Zhang *et al.* 2019a), and Cu formed an unstable heavy metal phosphate with phosphates, which increased the ecological risk of Cu. In the experimental group, with an increase of phosphate concentration, after adding GO, G-F and G-N-C stabilizers, the reduction of levels of dissolved oxygen in the G-F group was higher than that in the GO and G-N-C groups. G-F reduced the possibility of phosphate adhering to the surface of the sediment; furthermore, the efficiency of immobilizing Cu by G-F was higher than that by GO and G-N-C.

CONCLUSIONS

In this study, the effects of GO, G-F and G-N-C on immobilizing Cu in the sediments were compared. The results are discussed as follows. (1) Through the characterization of G-F and G-N-C, the results showed that the specific surface area of GO increased with the amount of Fe_3O_4 loaded, by grafting chitosan to GO, the number of surface functional groups increased and the structure became tight. (2) Increasing the mass fraction of the modified materials from 5% to 15%, the effect of immobilizing Cu in the sediments strengthened. (3) The efficiency of stable materials on immobilizing Cu from high to low is: G-F> G-N-C> GO. (4) Lower concentration of phosphates in the overlying water helped stabilize materials to reduce the ecological risk of Cu in the sediments. At the same concentration of phosphates in the overlying water, G-F had the best ability to immobilize Cu in the sediments, and it could be inferred that G-F could play a positive role in the treatment of phosphorus-rich water. G-F is a high-efficient and environmentally friendly material that can be used for contaminated site remediation. It is of great importance that the effect of eutrophication on the stability of heavy metals should also be taken into consideration.

ACKNOWLEDGEMENTS

This study was financially supported by the National Natural Science Foundation of China (No. 21107041); the Young and Middle-Aged Academic Backbone Program

of the Inner Mongolia University of Technology; the Natural Science Foundation of Inner Mongolia (No. 2020MS05028); the Department of Education of Inner Mongolia Autonomous Region (No. NJZY17095).

DATA AVAILABILITY STATEMENT

All relevant data are included in the paper or its Supplementary Information.

REFERENCES

Ahmad, S., Ahmad, A., Khan, S., Ahmad, S., Khan, I., Zada, S. & Fu, P. 2019 Algal extracts based biogenic synthesis of reduced graphene oxides (rGO) with enhanced heavy metals adsorption capability. *Journal of Industrial and Engineering Chemistry* **72**, 117–124.

Banks, J., Ross, D. J. & Keough, M. J. 2012 Short-term (24 h) effects of mild and severe hypoxia (20 and 5% dissolved oxygen) on metal partitioning in highly contaminated estuarine sediments. *Estuarine, Coastal and Shelf Science* **99**, 121–131.

Cao, Z. F., Wen, X., Wang, J., Yang, F., Zhong, H., Wang, S. & Wu, Z. K. 2019 In situ nano-Fe_3O_4/triisopropanolamine functionalized graphene oxide composites to enhance Pb^{2+} ions removal. *Colloids and Surfaces A: Physicochemical and Engineering Aspects* **561**, 209–217.

El-Shafai, N. M., Abdelfatah, M. M., El-Khouly, M. E., El-Shaerb, A., Mohamed, S. R., Mamdouh, S. M. & El-Kemarya, M. A. 2020 Magnetite nano-spherical quantum dots decorated graphene oxide nano sheet (GO@Fe_3O_4): electrochemical properties and applications for removal heavy metals, pesticide and solar cell. *Applied Surface Science* **506**, 144896.

Gil-Diaz, M., Diez-Pascual, S., Gonzalez, A., Alonso, J., Rodriguez-Valdes, E., Gallego, J. R. & Lobo, M. C. 2016 A nanoremediation strategy for the recovery of an as-polluted soil. *Chemosphere* **149**, 137–145.

Hu, Z. L., Qin, S. L., Zhi, H., Zhua, Y., Xia, L. J. & Li, Z. H. 2017 Recyclable graphene oxide-covalently encapsulated magnetic composite for highly efficient Pb(II) removal. *Journal of Environmental Chemical Engineering* **5**, 4630–4638.

Jiang, H. M., Zheng, X. P. & Li, W. 2018 Source and risk assessment of heavy metal in sediment of China. *China Population, Resources and Environment* **28**, 108–112.

Jin, Z., Ding, S., Sun, Q., Gao, S., Fu, Z., Gong, M., Lin, J., Wang, D. & Wang, Y. 2019 High resolution spatiotemporal sampling as a tool for comprehensive assessment of zinc mobility and pollution in sediments of a eutrophic lake. *Journal of Hazardous Materials* **364**, 182–191.

Liu, J. J., Diao, Z. H., Xu, X. R. & Xie, Q. 2019a Effects of dissolved oxygen, salinity, nitrogen and phosphorus on the release of heavy metals from coastal sediments. *Science of the Total Environment* **666**, 894–901.

Liu, X., Ma, R., Wang, X., Ma, Y., Yang, Y., Zhuang, L., Zhang, S., Jehan, R., Chen, J. & Wang, X. 2019b Graphene oxide-based materials for efficient removal of heavy metal ions from aqueous solution: a review. *Environmental Pollution* **252**, 62–73.

Lu, M., Luo, X., Jiao, J. J., Li, H. L., Wang, X. J., Gao, J. Y., Zhang, X. L. & Xiao, K. 2019 Nutrients and heavy metals mediate the distribution of microbial community in the marine sediments of the Bohai Sea, China. *Environmental Pollution* **255** (Pt 1), 113069.

Ramesha, G. K., Kumara, A. V., Muralidhara, H. B. & Sampath, S. 2011 Graphene and graphene oxide as effective adsorbents toward anionic and cationic dyes. *Journal of Colloid and Interface Science* **361** (1), 270–277.

Rinklebe, J., Shahee, N. S. M. & Frohne, T. 2016a Amendment of biochar reduces the release of toxic elements under dynamic redox conditions in a contaminated floodplain soil. *Chemosphere* **142**, 41–47.

Rinklebe, J., Shaheen, S. M. & Yu, K. 2016b Release of As, Ba, Cd, Cu, Pb, and Sr under pre-definite redox conditions in different rice paddy soils originating from the U.S.A. and Asia. *Geoderma* **270**, 21–32.

Samuel, M. S., Bhattacharya, J., Raj, S., Santhanam, N., Singh, H. & Pradeep Singh, N. D. 2019 Efficient removal of Chromium(VI) from aqueous solution using chitosan grafted graphene oxide (CS-GO) nanocomposite. *International Journal of Biological Macromolecules* **121**, 285–292.

Sanderson, P., Naidu, R. & Bolan, N. 2016 The effect of environmental conditions and soil physicochemistry on phosphate stabilisation of Pb in shooting range soils. *Journal of Environmental Management* **170**, 123–130.

Shi, Q., Zhang, S., Ge, J., Wei, J., Christodoulatos, C., Korfiatis, G. P. & Meng, X. 2020 Lead immobilization by phosphate in the presence of iron oxides: adsorption versus precipitation. *Water Research* **179**, 115853.

Shraban, K. S., Sandip, P., Biswal, S. K., Panda, B. B. & Hota, G. 2020 Fe_3O_4 nanoparticles functionalized GO/g-C_3N_4 nanocomposite: an efficient magnetic nanoadsorbent for adsorptive removal of organic pollutants. *Materials Chemistry and Physics* **244**, 122710.

Song, Z., Tang, W. & Shan, B. 2017 A scheme to scientifically and accurately assess cadmium pollution of river sediments, through consideration of bioavailability when assessing ecological risk. *Chemosphere* **185**, 602–609.

Su, X., Zhu, J., Fu, Q., Zuo, J., Liu, Y. & Hu, H. 2015 Immobilization of lead in anthropogenic contaminated soils using phosphates with/without oxalic acid. *Journal of Environmental Sciences (China)* **28**, 64–73.

Sun, C., Zhang, Z., Cao, H., Xu, M. & Xu, L. 2019 Concentrations, speciation, and ecological risk of heavy metals in the sediment of the Songhua River in an urban area with petrochemical industries. *Chemosphere* **219**, 538–545.

Wang, J., Cao, Z. f., Yang, F., Wang, S. & Zhong, H. 2018 Enhancement of catalytic performance by regulating the surface properties of Fe_3O_4 composites. *Journal of the Taiwan Institute of Chemical Engineers* **93**, 350–362.

Yadav, M., Rhee, K. Y., Park, S. J. & Hui, D. 2014 Mechanical properties of Fe_3O_4/GO/chitosan composites. *Composites Part B: Engineering* **66**, 89–96.

Yan, N., Liu, W., Xie, H., Gao, L., Han, Y., Wang, M. & Li, H. 2016 Distribution and assessment of heavy metals in the surface sediment of Yellow River, China. *Journal of Environmental Sciences (China)* **39**, 45–51.

Zeng, G., Wan, J., Huang, D., Hu, L., Huang, C., Cheng, M., Xue, W., Gong, X., Wang, R. & Jiang, D. 2017 Precipitation, adsorption and rhizosphere effect: the mechanisms for phosphate-induced Pb immobilization in soils-a review. *Journal of Hazardous Materials* **339**, 354–367.

Zhang, H. H., Cao, X. Y., Wang, H., Ma, Z., Li, J., Zhou, L. M. & Yang, G. P. 2019a Effect of black carbon on sorption and desorption of phosphorus onto sediments. *Marine Pollution Bulletin* **146**, 435–441.

Zhang, Q., Du, Z., Huang, X., Zhao, Z., Guo, T., Zeng, G. & Yu, Y. 2019b Tunable microwave absorptivity in reduced graphene oxide functionalized with Fe_3O_4 nanorods. *Applied Surface Science* **473**, 706–714.

Zhao, D., Yu, Y. & Chen, J. P. 2016 Treatment of lead contaminated water by a PVDF membrane that is modified by zirconium, phosphate and PVA. *Water Research* **101**, 564–573.

Zhao, J., Yang, Y., Li, C. & Hou, L. 2019 Fabrication of GO modified PVDF membrane for dissolved organic matter removal: removal mechanism and antifouling property. *Separation and Purification Technology* **209**, 482–490.

Zhuang, P., McBride, M. B., Xia, H., Li, N. & Li, Z. 2009 Health risk from heavy metals via consumption of food crops in the vicinity of Dabaoshan mine, South China. *Science of the Total Environment* **407** (5), 1551–1561.

First received 18 September 2019; accepted in revised form 4 August 2020. Available online 17 August 2020